Thermotropic and lyotropic phase behaviour of monoalkyl glycosides

P. Sakya; J. M. Seddon

PLEASE SCROLL DOWN FOR ARTICLE

Thermotropic and lyotropic phase behaviour of monoalkyl glycosides

by P. SAKYA†, J. M. SEDDON*

Department of Chemistry, Imperial College, Exhibition Road, London SW7 2AY,
U.K.

and V. VILL

University of Hamburg, Institute of Organic Chemistry, Martin-Luther-
King Platz 6, D-20146 Hamburg 13, Germany

We have studied the thermotropic and lyotropic phase behaviour of seven monoalkyl glycosides using polarizing microscopy, differential scanning calorimetry and X-ray diffraction. The phase behaviour of these non-ionic surfactants is compared with that of two previously studied monoalkyl glycosides [1]. We have found that small modifications in chemical structure can lead to large changes in the phase behaviour. The results reveal the effect of changes in alkyl glycoside chemical structure on the phase behaviour, in particular, on the melting point, the clearing point, the solubility in water, and the extent of the lamellar and curved phases. Seven out of the nine surfactants were found to exhibit thermotropic mesomorphism. Furthermore, in the presence of water, three formed lamellar (L_α), type I cubic (Q_I) and type I hexagonal (H_I) phases, two formed lamellar and cubic phases, and two formed only lamellar phases. The cubic phase in each case was indexed, either from powder-like or monodomain samples, as spacegroup $Ia3d$. The lowest order low angle X-ray spacings were found to lie on single, continuous lines with varying water content across the L_α, Q_I and H_I phases, implying epitaxial relationships between these phases at the phase boundaries.

1. Introduction

A study of the phase behaviour of two monoalkyl glycosides, *n*-octyl 1-*O*-*β*-D-glucopyranoside and its thio derivative *n*-octyl 1-*S*-*β*-D-glucopyranoside, has previously been published [1]. In this paper we have studied seven other monoalkyl glycosides, all of whose structures can be considered to be based on that of *n*-octyl 1-*O*-*β*-D-glucopyranoside. By comparing the phase behaviour of all nine molecules we hope to gain a more thorough understanding of the relationship between molecular structure and phase behaviour.

Figure 1 lists the chemical structures of all nine surfactant molecules. A variety of different nomenclatures has been used previously for the alkyl glycosides. For example, the name of the compound *n*-octyl 1-*O*-*β*-D-glucopyranoside has been variously abbreviated to *β*OG [1, 2], OOG [3] and C_8G_1 [4]. In order to indicate all the aspects of the chemical structure which will be studied in this paper, we will use the new abbreviation

β-C_8Glc. The '*β*' denotes that the chain group is equatorial to the sugar ring, whereas an '*α*' would indicate that the chain group is axial to the sugar ring; the C_8 denotes the presence of an alkyl chain with eight carbon atoms; the 'Glc' denotes a glucopyranoside head group. Similarly, 'Fuc' stands for fucopyranoside, 'Man' for mannopyranoside, and 'Gal' for galactopyranoside. A 'thio' is added if the atom linking the sugar head group to the alkyl chain (the bridging atom) is sulphur rather than oxygen (e.g. thio-*β*-C_8Glc).

All the compounds studied here are based on a pyranoside ring of five carbons and an oxygen, linked to an alkyl chain by either an oxygen or a sulphur atom. The glucose, fucose and galactose rings differ in the precise arrangement of the substituents at different sites on the ring. All of the compounds contain hydroxyl groups bonded to C2, C3 and C4 on the sugar ring. On the glucopyranoside ring all these hydroxyls are equatorial. In the fucopyranoside and galactopyranoside rings the OH group on C4 is axial, while the others are equatorial. In the mannopyranoside ring the C2 hydroxyl group is axial while the others are equatorial. In the case of the glucopyranosides, the mannopyranos-

†Current address: Unilever Research, Port Sunlight Laboratory, Quarry Road East, Bebington, Wirral, Merseyside L63 3JW, U.K.
*Author for correspondence.

n-octyl 1-*O*-α-D-glucopyranoside (α-C$_8$Glc)
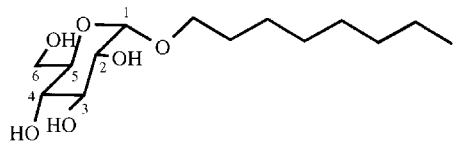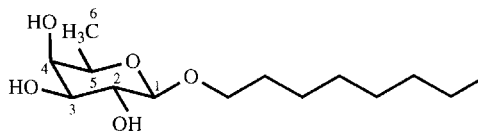
n-octyl 1-*O*-β-D-fucopyranoside (β-C$_8$Fuc)

n-octyl 1-*O*-β-D-glucopyranoside (β-C$_8$Glc)
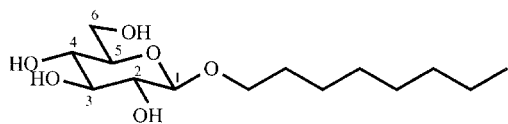
n-octyl 1-*O*-α-D-mannopyranoside (α-C$_8$Man)
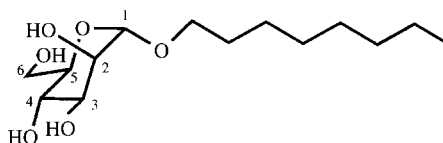
n-octyl 1-*S*-β-D-glucopyranoside (thio-β-C$_8$Glc)
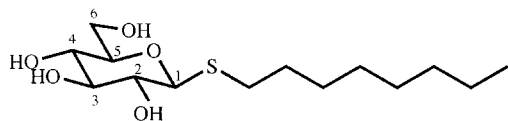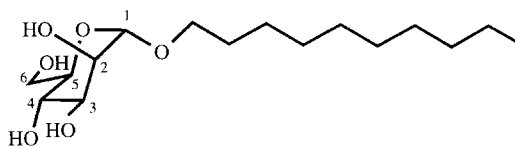
n-decyl 1-*O*-α-D-mannopyranoside (α-C$_{10}$Man)

n-octyl 1-*O*-β-D-galactopyranoside (β-C$_8$Gal)
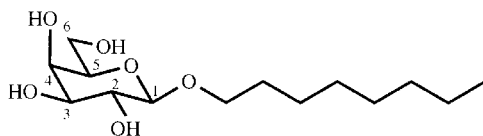
n-dodecyl 1-*O*-α-D-mannopyranoside (α-C$_{12}$Man)
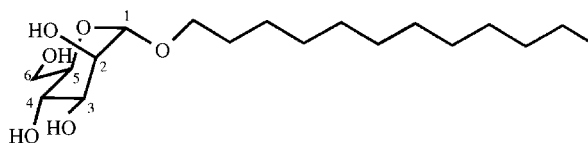
n-octyl 1-*O*-α-D-fucopyranoside (α-C$_8$Fuc)
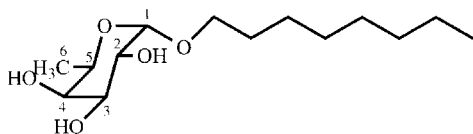
Figure 1. Chemical structures of the nine monoalkyl glycosides. Note that the fucopyranosides studied were actually the L-isomers, but are shown here in the D-configuration to emphasize their structural relationships to the other alkyl glycosides.

ides and the galactopyranosides, there is an equatorial CH$_2$OH group on C5 of the sugar ring. In the fucopyranosides this is replaced by an equatorial CH$_3$ group. With the exceptions of α-C$_{10}$Man and α-C$_{12}$Man, the alkyl chain is always eight carbons long. For all the compounds studied here, the sugar group was in the D-configuration, apart from the fucopyranosides, which were the L-isomers.

There has been a rapid growth in the study of glycoside surfactants as liquid crystalline mesogens in recent years.

Alkyl glycosides constitute a large class of *thermotropic* liquid crystals. The growth of research in this field over recent years has been extensively reviewed [5–7]. A number of cyclic and acyclic glycosides with single *n*-alkyl or *n*-acyl chains of more than six carbon atoms are known to form smectic, probably A_d (interdigitated bilayer), phases.

The thermotropic properties of β-C_8Glc have been studied by several authors. Goodby [8] studied aligned samples of the liquid crystalline mesophase and concluded that it is likely to be of the smectic A_d type. The thermotropic phase behaviour of binary mixtures of the α and β-glucopyranosides has also been studied, and the two anomers compared [9]. A summary of the thermotropic transition temperatures of a number of single-chain alkyl glycosides has been given by Vill *et al.* [10]. The thermotropic behaviour of a related class of amino linked compounds including the *n*-alkyl 1-amino β-D-glucopyranosides has also been published [11].

Most of the alkyl glycosides that exhibit thermotropic behaviour also possess *lyotropic* properties [6, 12], and much current research is focused on their use as surfactants. For example, *n*-octyl 1-*O*-β-D-glucopyranoside is frequently used to solubilize membrane proteins [13, 14]. In addition, a comparison of the surfactant properties of glycoside and polyoxyethylene surfactants [15] has shown that alkyl glycosides possess both stronger hydrophilicity and stronger lipophobicity than equivalent polyoxyethylene surfactants. Moreover, alkyl glycosides can be derived from renewable resources and are more biodegradable than their polyoxyethylene analogues. The surface activities, biodegradability and antimicrobial properties of a range of single-chain glycosides have been studied [16]. There is thus a large scope for the use of glycoside surfactants in a broad range of industrial applications, such as emulsification, detergency and pharmaceutical formulations.

To be usable as surfactants, alkyl glycosides must be sufficiently soluble in water. Several compounds that form smectic A_d mesophases when dry have, indeed, been found to form fluid lamellar $L\alpha$ phases on the addition of water. Chung and Jeffrey [2] have analysed the lyotropic properties of a number of *n*-alkyl pyranosides, and they found that β-C_8Glc, in particular, exhibits a fluid lamellar phase $L\alpha$ at low hydrations, and type I cubic Q_I and hexagonal H_I phases at higher hydrations. On further addition of water a micellar solution is formed. They identified the space group of the cubic phase as *Fm3m*. In addition, Loewenstein *et al.* [17–19] have used deuterium NMR to study the phase behaviour of the *n*-alkyl α- and *n*-alkyl β-D-glucopyranosides, including β-C_8Glc, both with water (D_2O) and also with several non-aqueous solvents.

In a previous paper, we reported the thermotropic and lyotropic phase behaviour of β-C_8Glc and its thio derivative thio-β-C_8Glc in water [1]. Dry β-C_8Glc was found to form a crystalline lamellar L_c phase with a layer spacing of 29·3 Å which is stable up to 69°C, and a smectic A_d phase which is stable up to 107°C and whose layer spacing ranges from 25·6 Å (70°C) to 25·3 Å (105°C). We confirmed the results of Chung and Jeffrey [2] that β-C_8Glc forms the lamellar, cubic and hexagonal phases, but we found that the cubic phase is of space group *Ia3d*, not *Fm3m* as they had reported.

The L_c phase of dry thio-β-C_8Glc was found to be stable up to 42°C, with a layer spacing of 32·3 Å, whereas the smectic A_d phase is stable up to 126°C and has a layer spacing of 26·2 Å. Thus the smectic phase of thio-β-C_8Glc exists over a much wider temperature range than that of β-C_8Glc. We found that thio-β-C_8Glc also forms the lamellar and *Ia3d* cubic phases in water, but no hexagonal phase.

Our results for the β-C_8Glc/water system have recently been confirmed by Nilsson *et al.* [4], who reported a similar phase diagram, and also concluded that the space group of the cubic phase is most likely to be *Ia3d*.

The phase behaviour exhibited by β-C_8Glc is quite similar to that of the polyoxyethylene system $C_{12}EO_6$/water [20]. The epitaxial relationships in this latter system have been studied in some depth [21–24]. The main conclusion was that the (0 0 1) planes of the lamellar phase transform into the (2 1 1) planes of the *Ia3d* cubic phase, which in turn become the (1 0) planes of the hexagonal phase. If these epitaxial relationships also apply to the β-C_8Glc/water system, then one would expect the d_{001} spacing of the lamellar phase to be equal to the d_{211} spacing of the cubic phase, and the d_{211} cubic spacing to match the d_{10} spacing of the hexagonal phase, at the respective phase boundaries; we found this to be the case [1].

The thermotropic properties of some of the other seven compounds examined in this chapter have been previously studied [10], but very little work has so far been published on their lyotropic phase behaviour. We have therefore examined these compounds to determine their lyotropic phase behaviour, and to compare it with that of β-C_8Glc and thio-β-C_8Glc.

2. Experimental

The alkyl gluco-, galacto- and mannopyranosides studied here were synthesized by a general procedure which has been described by Vill *et al.* [10], and the fucopyranosides, synthesized according to reference [25], were a gift from Dr. T. Lindhorst. The products were found to be ≥99% pure by NMR and thin layer chromatography.

The first step in analysing the glycoside surfactants was to examine their thermotropic properties. This was

done by the use of a Nikon Labophot polarizing micro-scope with a Linkam heating stage. Thermotropic phase transition temperatures (estimated accuracy $\pm 1°C$) were measured by both polarizing microscopy and differential scanning calorimetry (Perkin-Elmer DSC-2C).

The second step was to analyse the lyotropic phase behaviour of each alkyl glycoside. A water penetration scan was first performed on a sample of the compound, as described by Chung and Jeffrey [2]. In order to construct detailed phase diagrams of the compounds, a number of samples of precise composition were prepared. The proportion of water in each sample ranged from approximately 5 to 40 wt %, and samples were prepared at approximately 3–4 wt % water intervals.

The required amounts of compound and water were weighed in Lindemann glass X-ray capillary tubes (dia-meter 1·5 mm). The uncertainty in the concentration of the surfactant, $\Delta c/c$, is estimated to be 1–2 wt %. Approximately 7–12 mg of the compound, in the form of a fine polycrystalline powder, was added and centri-fuged to the base of the tube. The required mass of water was added using a very fine glass pipette and centrifuged down, and the tube was then sealed.

The lyotropic phases could be distinguished from each other by polarizing microscopy. The cubic phase is optically isotropic and black, whereas both the lamellar and hexagonal phases are birefringent. However, the hexagonal phase tends to form much larger domains than the lamellar phase, and exhibits a characteristic mosaic structure. To distinguish the cubic and micellar phases, which are both isotropic under the polarizing microscope, the shape of the air bubbles trapped within the phases was examined. Bubbles present in the cubic phase were 'frozen' into fixed positions and tended to develop faceting, whereas bubbles in the micellar phase were spherical and free to diffuse about. Above room temperature ($22 \pm 1°C$), points on the phase boundaries were found by heating the capillary samples using the heating stage of the polarizing microscope and observing any phase transitions.

To observe phase transitions below room temperature, X-ray diffraction was used. Samples were cooled by Peltier temperature control on the X-ray beamline and changes in the diffraction pattern were noted. X-ray diffraction was also used to obtain layer spacings and lattice parameters, and to identify the space groups of the cubic phases. The X-rays were produced by a GX20 rotating anode X-ray generator (Enraf-Nonius, Netherlands) operating at 30 kV and 25 mA, with a 100 μm focus cup, and were focused by Franks optics to a point of dimensions $160 \times 110 \, \mu m^2$. This was used in conjunction with a custom-built electronic two-dimensional CCD detector which allows the capture of X-ray diffraction images in 60 seconds or less. The

images produced could be processed and indexed from a single computer terminal. The estimated accuracy of the measured layer spacings was $\pm 0·5$ Å.

3.   Results
3.1.   *n-Octyl 1-O-α-D-glucopyranoside (α-C$_8$Glc)*

The crystalline solid *n*-octyl 1-*O*-α-D-glucopyranoside melted at 69°C to form a smectic phase which was stable up to 116°C (compared with literature values of 71·8°C and 118°C [10]). There was insufficient sample to take X-ray diffraction measurements, but Dorset [9] gives values of 19·7 Å for the layer spacing of the L_c phase at 25°C, and 23·3 Å for the smectic phase layer spacing at 75°C.

α-C$_8$Glc is insoluble in water, so a penetration scan at room temperature on a sample of the solid surfactant could not be made. However, when the surfactant was heated into the smectic phase and water added, a fluid lamellar L_α phase was observed to form.

3.2.   *n-Octyl 1-O-β-D-galactopyranoside (β-C$_8$Gal)*

β-C$_8$Gal differs in structure from β-C$_8$Glc only in that the C4-linked hydroxyl group is axial rather than equat-orial. Nonetheless, this change is sufficient to cause the smectic A_d phase to be stable in a considerably more elevated temperature range than the mesophase of β-C$_8$Glc. The solid melted at 96°C, and the smectic phase was stable up to 127°C. This compares with literature values of 98·3°C and 132·9°C [10].

The crystalline lamellar phase of β-C$_8$Gal has a bilayer spacing of 25·1 Å, smaller than the value of 29·3 Å for β-C$_8$Glc. However, the *d*-spacing of the β-C$_8$Gal smectic A phase, 25·8 Å, is similar to the corresponding value for β-C$_8$Glc.

The phase diagram of β-C$_8$Gal is given in figure 2. It is similar to the phase diagram previously found for β-C$_8$Glc [1], with the L_α, Q_I and H_I phases present, although the cubic phase exists over a slightly narrower composition range, and the hexagonal phase is stable to a higher temperature and over a wider range of composi-tions. As for the previously studied β-C$_8$Glc system [1], the cubic phase indexes as space group *Ia3d*. The biggest difference between β-C$_8$Gal and β-C$_8$Glc is the much greater temperature stability of the crystalline lamellar phase for the latter system. Even at high hydrations, a lamellar L_β gel phase always forms at room temperature, and is stable up to 42°C. To access the fluid lyotropic phases of fixed composition samples, these samples had to be heated above 42°C, though it was found that when the samples were cooled back to room temperature the lyotropic phases, especially the cubic phase, often continued to exist as supercooled phases.

The L_α phase has a *d*-spacing of between 26·5 Å (8 wt % water) and 28·2 Å (13 wt % water). The Q_I phase
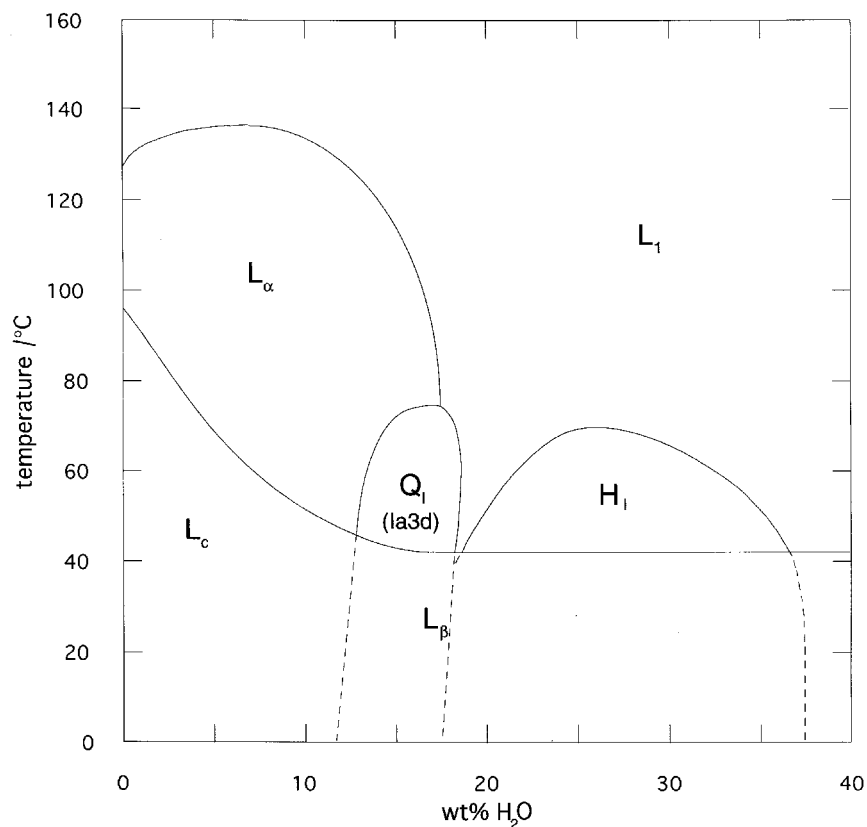
Figure 2. Binary phase diagram of β-C_8Gal in water; the dashed lines indicate regions where supercooling occurs.

lattice parameter varies between 69·1 Å (15 wt % water) and 70·8 Å (17 wt % water), and the H_I phase lattice parameter ranges from 34·8 Å (22 wt % water) to 36·7 Å (32 wt % water). The values for the layer spacings and lattice parameters are close to, but slightly smaller than, those of the equivalent β-C_8Glc phases. The variation of the lowest angle d-spacing with hydration is shown in figure 3. The d-spacing increases smoothly with

increasing hydration across the three phases, implying epitaxial relationships between the phases.

3.3. *n-Octyl 1-O-α-L-fucopyranoside (α-C_8Fuc)*

It was found that *n*-octyl 1-*O*-α-L-fucopyranoside is insoluble in water at room temperature, and on heating the solid, it remained crystalline up to 110°C, at which point a micellar solution formed. No lyotropic liquid
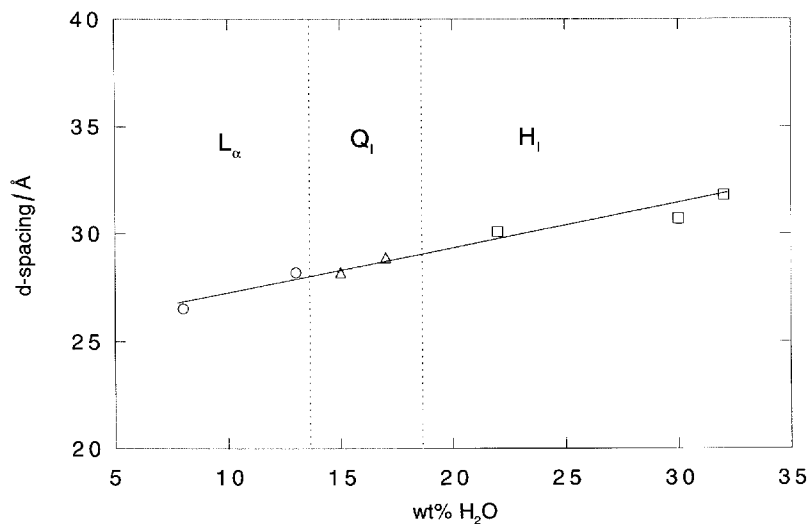
Figure 3. Plot of d-spacing versus water content at 50°C for β-C_8Gal. The L_α (d_{001}), Q_I (d_{211}) and H_I (d_{10}) phases are represented by circles, triangles and squares, respectively. Dotted lines indicate phase boundaries at 50°C.

crystalline phases were observed. The layer spacing of the crystalline lamellar phase, at 17·4 Å, is roughly the length of the α-C$_8$Fuc molecule. This suggests that the molecules pack in monolayers rather than bilayers.

3.4. *n-Octyl 1-O-β-L-fucopyranoside (β-C$_8$Fuc)*

n-octyl 1-*O*-β-L-fucopyranoside was also found to be insoluble in water at room temperature, and remained crystalline on heating up to 73°C, at which point a micellar solution formed. No lyotropic phases were observed.

3.5. *n-Octyl 1-O-α-D-mannopyranoside (α-C$_8$Man)*

α-C$_8$Man differs in structure from α-C$_8$Glc only in that the C2-linked hydroxyl group is axial rather than equatorial. Like α-C$_8$Glc it forms a smectic A$_d$ phase on heating. The mesophase exists over a wider temperature range than for α-C$_8$Glc, with a melting point of 58°C, and a clearing point of 132°C. These figures are close to the literature values of 55·0°C and 133·9°C [10]. The change in configuration of the C2-linked hydroxyl from equatorial to axial thus appears to stabilize the smectic phase.

The bilayer spacing of the crystalline lamellar phase is 23·5 Å, and that of the smectic phase is 23·1 Å. These results, plus those for α-C$_8$Glc, show that the layer

spacings of the α-anomers are generally smaller than those of the β-anomers.

Unlike α-C$_8$Glc and α-C$_8$Fuc, α-C$_8$Man was found to exhibit extensive lyotropic phase behaviour. The binary phase diagram is given in figure 4. When water is added, α-C$_8$Man forms a fluid lamellar L$_\alpha$ phase, a cubic phase and a hexagonal phase. The phase behaviour is similar to that of β-C$_8$Glc and β-C$_8$Gal, but the cubic phase exists over a wider range of hydrations, and at higher temperatures the region of cubic phase stability is tilted towards higher hydrations. Although a monodomain diffraction pattern of the cubic phase was not obtained, powder diffraction patterns showed strong $\sqrt{6}$ and $\sqrt{8}$ reflections and a medium intensity $\sqrt{14}$ reflection, which is characteristic of the *Ia3d* cubic phase.

The lamellar phase has a layer spacing of 24·3 Å. The lattice parameter values for the Q$_I$ phase range from 65·0 Å (14 wt % water) to 68·5 Å (18 wt % water), and those for the H$_I$ phase range from 32·8 Å (22 wt % water) to 35·4 Å (30 wt % water). As with the smectic and lamellar phases, the cubic phase and the hexagonal phase values are both smaller than for β-C$_8$Glc or β-C$_8$Gal. The variation of *d*-spacing with hydration, shown in figure 5, is roughly linear, gently increasing and continuous across the phase boundaries, implying epitaxial relationships between the phases.
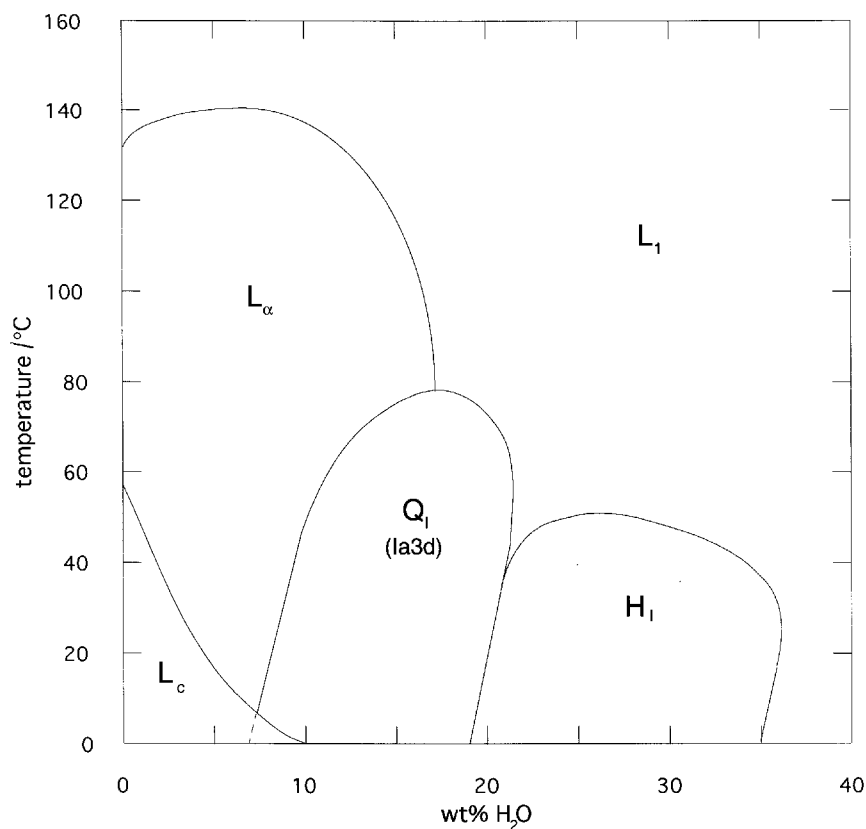

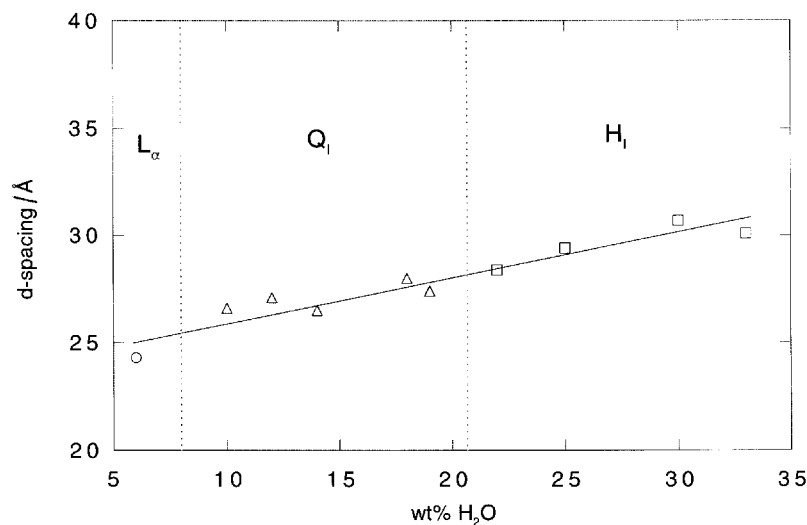Figure 4.   Binary phase diagram of α-C$_8$Man in water; the dashed line indicates a region where supercooling occurs.

Figure 5. Plot of *d*-spacing versus water content at 22°C for α-C_8Man. The L_α (d_{001}), Q_I (d_{211}) and H_I (d_{10}) phases are represented by circles, triangles and squares, respectively. The dotted lines indicate the phase boundaries at this temperature.

3.6. *n-Decyl 1-O-α-D-mannopyranoside (α-C_{10} Man)*

In order to examine the effect of alkyl chain length on phase behaviour, the C_{10} and C_{12} homologues of α-C_8Man, *n*-decyl 1-*O*-α-D-mannopyranoside (α-C_{10}Man), and *n*-dodecyl 1-*O*-α-D-mannopyranoside (α-C_{12}Man), were also studied.

α-C_{10}Man formed a smectic A_d phase over a wider and more elevated temperature range than α-C_8Man, with a melting point of 62°C, and a clearing point of 149°C (compared with literature values of 64·7°C and 152·7°C [10]).

The bilayer spacing of the crystalline lamellar phase was not totally clear, as a weak inner diffraction ring gave a spacing of 22·0 Å, whereas a stronger outer ring gave a spacing of 27·2 Å. The smectic A_d layer spacing was 26·4 Å, an increase of 3·3 Å over α-C_8Man.

The binary phase diagram is given in figure 6. The compound forms an L_α phase at low hydrations, and an *Ia3d* Q_I phase at higher hydrations, with no H_I phase present. The phase behaviour is very similar to that of thio-β-C_8Glc. In the case of α-C_{10}Man, the Q_I phase is stable over a slightly wider range of hydrations, and the L_α, Q_I and L_c phases are all stable to higher temperatures. Even at high hydrations the L_β gel phase was stable up to 10°C.

Figure 7 (*a*) shows the diffraction pattern of an aligned α-C_{10}Man/32 wt % water sample. The Bragg peaks are sharp, with little arcing, indicating that this is a well aligned sample (close to a monodomain). There is comparatively little diffuse scatter, indicating that the structure elements within the cubic phase have relatively little displacement disorder [22]. The pattern exhibits 21 Bragg peaks which are indexed in figure 7 (*b*) as cubic space group *Ia3d* (the indexing of monodomain cubic phases is described in greater detail in [1]). This corresponds to six independent orders of reflection (because of the wide range in intensity of the peaks, the 21 peaks are not all clearly visible in the print out). The pattern corresponds to a section in reciprocal space normal to the [1 1 1] axis of the cubic lattice. Table 1 compares the measured reciprocal spacing for each *h k l* reflection with that calculated for an *Ia3d* cubic lattice with $a = 83·2$ Å. The fit between the theoretical and observed spacings is good (note that the agreement between the calculated and observed spacings from aligned diffraction patterns is normally less perfect than that from powder patterns, due to slight misalignment effects); furthermore, the variation in peak intensity is very similar to that of β-C_8Glc [1].

The measured layer spacing for the L_α phase was 28·2 Å, and lattice parameters for the Q_I phase were in the range 76·7 Å (14 wt % water) to 84·9 Å (25 wt % water). The lattice parameter values for the Q_I phase are the largest for any of the alkyl glycosides studied here, being slightly larger than the values for the thio-β-C_8Glc cubic phase, and 15–20% larger than the values for the α-C_8Man cubic phase. The variation of *d*-spacing with hydration, shown in figure 8, is again linear, implying epitaxial relationships between the phases, and increases with increasing hydration.

3.7. *n-Dodecyl 1-O-α-D-mannopyranoside (α-C_{12} Man)*

n-dodecyl 1-*O*-α-D-mannopyranoside (α-C_{12}Man) formed a smectic A_d phase over a wider and more elevated temperature range than α-C_{10}Man, with a melting point of 67°C, and a clearing point of 157°C (compared with literature values of 74·2°C and 161·7°C [10]). Drawing together the results of the three mannopyranoside compounds, we see that, as expected, increasing
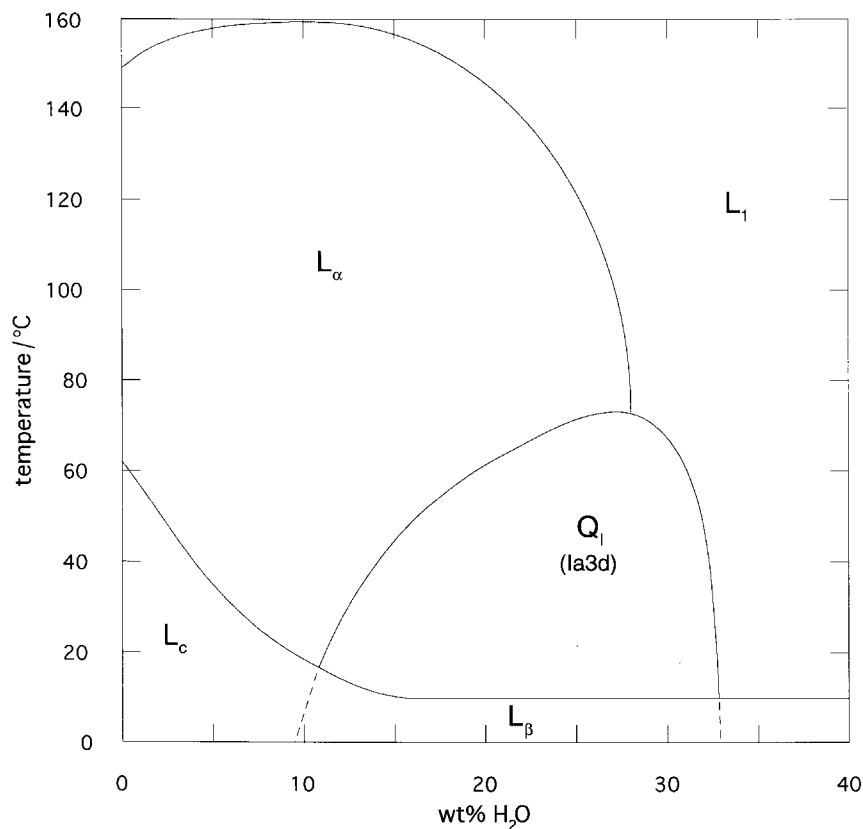
Figure 6. Binary phase diagram of
α-C_{10}Man in water; the dashed
lines indicate regions where
supercooling occurs.

alkyl chain length stabilizes both the crystalline and
smectic phases.

The bilayer spacing of the crystalline lamellar phase
of α-C_{12}Man was 24.8 Å, and that of the smectic phase
was 28.9 Å, an increase of 2.5 Å over its C_{10} analogue.

In the presence of water, the chain-melting transition
temperature of α-C_{12}Man fell with increasing water
content to a limiting value of $43°C$. Above the chain-
melting transition, it was found to form only the $L\alpha$
phase, but no Q_I or H_I phases. The $L\alpha$ layer spacings
ranged from 36.5 Å (30 wt % water) to 39.5 Å (40 wt %
water).

4.   Discussion

The results of this comparative study show that even
very small changes in the chemical structure of alkyl
glycosides can produce large variations in their thermo-
tropic and lyotropic phase behaviour. In order to aid
comparison, the melting and clearing points of the dry
compounds, plus the highest temperatures to which the
$L\alpha$, Q_I and H_I phases are stable, are given in table 2.
Dashes indicate that the phase does not exist for the
compound in question. In addition, table 3 lists the layer
spacings of the L_c and SmA phases, and table 4 summar-
izes the layer spacings of the $L\alpha$ phase and the lattice
parameters of the Q_I and H_I phases.

Of the nine alkyl glycosides studied, seven formed a
thermotropic (SmA) mesophase, with melting points
ranging from $42°C$ to $110°C$, and clearing points in the
range $107°C$ to $157°C$. Six of these compounds also
exhibited lyotropic phase behaviour. For comparison,
figure 9 shows the previously published phase diagrams
[1] of β-C_8Glc/water and thio-β-C_8Glc/water, along
with the three phase diagrams presented here (figures 2,
4 and 6). We can see that the fluid lamellar $L\alpha$ phase
occurs in all of the diagrams, the cubic phase is present
in all five diagrams, and the hexagonal H_I phase is
additionally present in three of the systems.

The single common feature of the five phase diagrams
is that all the curved phases which form are of type I
(oil-in-water), because of the large size of the polar head
group relative to the non-polar chain group. But, this
restriction apart, the variety of phase behaviour pro-
duced is quite large.

4.1.   *Thermotropic properties of the dry alkyl glycosides*
4.1.1.   *Melting point*

The melting transition for each of the dry alkyl
glycosides corresponds to a transition from a crystalline
lamellar phase to a liquid crystalline smectic A phase.
To understand the melting process, we must first examine
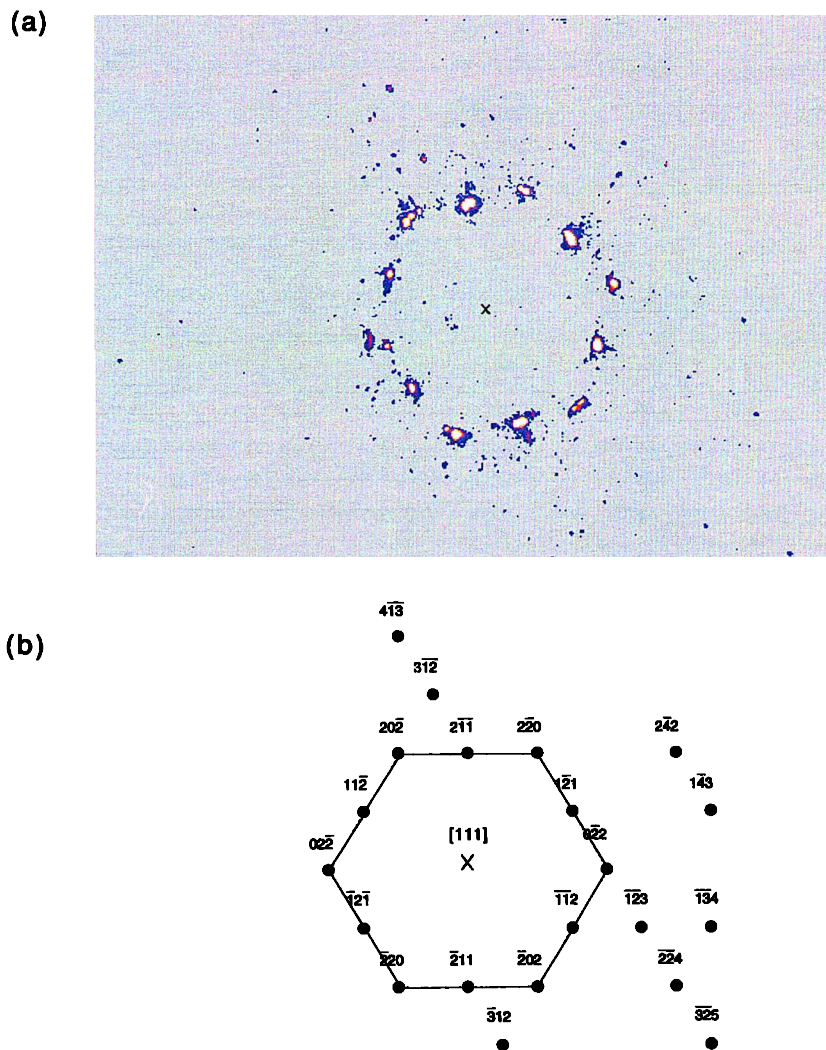the structures of these phases.

(a)

(b)

Figure 7. (*a*) X-ray diffraction pattern for a α-C_{10}Man/32 wt % water cubic phase sample at 22°C. (*b*) Indexing of the pattern.

Table 1. X-ray diffraction data for α-C_{10}Man/32 wt % water at 22°C. The s_{obs} are the observed reciprocal spacings and s_{cal} are the reciprocal spacings calculated for a *Ia3d* cubic lattice with $a = 83.2$ Å. The reflections correspond to the diffraction pattern shown in figure 7. I_{obs} are the intensities observed at the maximum of each peak. If there was more than one Bragg peak per order of reflection, the mean of the peak intensities was taken.

$h\,k\,l$	$h^2 + k^2 + l^2$	s_{obs} /10^{-3} Å^{-1}	I_{obs}	s_{cal} /10^{-3} Å^{-1}
211	6	29·9	7347	29·4
220	8	34·7	3202	34·0
321	14	45·0	433	45·0
422	24	56·4	369	58·9
431	26	61·7	599	61·3
440	32	75·4	418	74·1

Crystal structure determination is required to reveal the interactions between molecules in the crystalline state. The crystal structure of the relatively insoluble *n*-octyl 1-*O*-α-D-glucopyranoside has been obtained [26, 27]. However, it is a source of frustration to us that the crystal structures of all the other glycosides examined here, in particular β-C_8Glc, remain unknown. The high solubility of β-C_8Glc means that it has not, as yet, been possible to obtain single crystals of sufficient size and quality to enable its X-ray structure to be solved.

Jeffrey has, instead, succeeded in obtaining crystal structures for both α-C_8Glc and β-C_8Glc from 1:1 binary mixtures of the two anomers [28]. The crystal structure of thio-α-C_7Man (*n*-heptyl 1-*S*-α-mannopyranoside) has also been obtained [29]. In both these structures, and indeed in all the other glycoside crystal structures which have been solved, the molecules pack to form head-to-head bilayer structures with interdigitated chains.
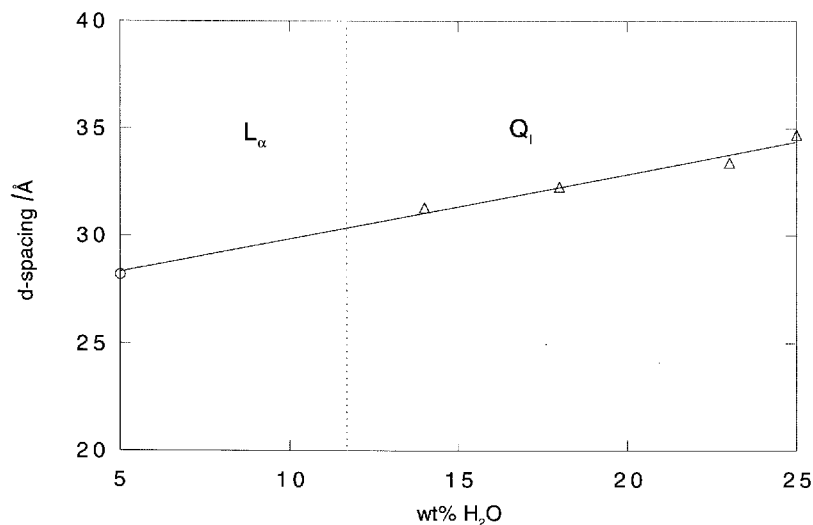
Figure 8.   Plot of *d*-spacing versus water content at 22°C for α-C_{10}Man. The $L\alpha$ (d_{001}) and Q_I (d_{211}) phases are represented by circles and triangles, respectively. The dotted line indicates the phase boundary at this temperature.

Table 2.   Melting points (T_m) and clearing points (T_c) of the dry compounds, and the highest temperatures at which the $L\alpha$, Q_I and H_I phases are stable.

Compound	Thermotropic behaviour		Lyotropic behaviour		
	T_m/°C	T_c/°C	$L\alpha$/°C	Q_I/°C	H_I/°C
α-C_8Glc	69	116	Not known	—	—
β-C_8Glc	69	107	122	62	32
thio-β-C_8Glc	42	126	136	68	—
β-C_8Gal	96	127	136	75	70
α-C_8Fuc	110		No thermotropic or lyotropic phases		
β-C_8Fuc	73		No thermotropic or lyotropic phases		
α-C_8Man	58	132	140	78	51
α-C_{10}Man	62	149	159	73	—
α-C_{12}Man	67	157	166	—	—

Table 3.   Thermotropic behaviour; layer spacings of the dry compounds.

Compound	Crystalline lamellar, L_c (25°C)	Smectic, SmA	
	d/Å	*d*/Å	*T*/°C
α-C_8Glc	19·7[a]	23·3[a]	75
β-C_8Glc	29·3	25·6/25·3	70/105
thio-β-C_8Glc	32·3	26·2	90
β-C_8Gal	25·1	25·8	90
α-C_8Fuc	17·4	No thermotropic phases	
β-C_8Fuc	Not known	No thermotropic phases	
α-C_8Man	23·5	23·1	90
α-C_{10}Man	22·0/27·2	26·4	90
α-C_{12}Man	24·8	28·9	90

[a] Values taken from reference [9].

The arrangement of molecules in the 1:1 binary mixture of α-C_8Glc and β-C_8Glc (figure 10) [28] is typical of the crystal structure of monoalkyl glycosides. Bilayers form, with the polar head groups on the outside and the interdigitated, non-polar chain groups on the inside. The head groups hydrogen bond both to the head groups on the opposing layer, and to adjacent head groups in the same layer, forming a strong hydrogen

Table 4. Lyotropic behaviour; layer spacings of the L_α phase and lattice parameters of the Q_I and H_I phases. Measurements were taken at 25°C except for β-C_8Gal and α-C_{12}Man, for which they were taken at 50°C.

Compound	L_α d/Å	Q_I a/Å	H_I a/Å
α-C_8Glc	Not known	—	—
β-C_8Glc	26·6–29·7 (5–19 wt % H_2O)	73·0 (22 wt % H_2O)	38·6 (33 wt % H_2O)
Thio-β-C_8Glc	27·8 (4–6 wt % H_2O)	74·1–78·8 (13–25 wt % H_2O)	—
β-C_8Gal	26·5–28·2 (8–13 wt % H_2O)	69·1–70·8 (15–17 wt % H_2O)	34·8–36·7 (22–32 wt % H_2O)
α-C_8Fuc		No lyotropic phases	
β-C_8Fuc		No lyotropic phases	
α-C_8Man	24·3 (6 wt % H_2O)	65·0–68·5 (10–19 wt % H_2O)	32·8–35·4 (22–33 wt % H_2O)
α-C_{10}Man	28·2 (5 wt % H_2O)	76·7–84·9 (14–25 wt % H_2O)	—
α-C_{12}Man	36·5–39·5 (25–45 wt % H_2O)	—	—

bonded network. The chain groups are held in place by weaker van der Waals interactions with adjacent chain groups. When the solid is heated, these chains 'melt', disengaging from the crystal lattice, but hydrogen bonding between the head groups maintains the bilayer structure, forming a smectic A phase [30, 31]. The alkyl chains are disordered, and the molecules can rotate about their long axes. The hydrogen bonding between head groups is dynamic rather than static. It is only at a much higher temperature, the clearing point, that the hydrogen bonding is also broken, and an isotropic, disordered liquid is formed.

It is the stability of the crystalline phase relative to the smectic phase which determines the melting point. There are two main factors which affect crystalline stability and thus the melting point.

4.1.1.1. Degree of interdigitation of the alkyl chains

The melting point of β-C_8Gal is 27°C higher than that of β-C_8Glc, whereas the melting point of thio-β-C_8Glc is 27°C lower than that of its oxygen-linked analogue. Differences in the layer spacings of these compounds imply that their crystal packing differs. The lamellar crystalline L_c phase of β-C_8Gal has a smaller layer spacing (25·1 Å) than that of β-C_8Glc (29·3 Å), whereas the L_c phase of thio-β-C_8Glc has a larger layer spacing (32·3 Å). Yet all three molecules have very similar chemical structures (figure 1), and their layer spacings in the smectic phase are almost identical (25·8 Å for β-C_8Gal, 25·3–25·6 Å for β-C_8Glc and 26·2 Å for thio-β-C_8Glc). It appears that it is the differences in crystal packing which lead to changes in melting point. Without the full crystal structures of the three compounds we cannot ascertain

precisely what these differences are. But we suggest that the decrease in crystal layer spacing may be due to a greater degree of interdigitation of the alkyl chains. The greater the interdigitation, the greater the interactions between neighbouring alkyl chains and the higher the melting point.

4.1.1.2. Chain length

As expected, the melting point increases progressively in the α-C_xMan homologous series (with $x = 8$, 10 or 12) as the alkyl chain length is increased. This is because the longer the chain, the stronger the van der Waals interactions between them, and the greater is the energy required to melt them. A similar increase has been found for the α-C_xGlc and β-C_xGlc homologous series [32]. A slight odd–even effect has also been observed for the α-C_xGlc series, with melting points for the even chain lengths being higher than those for the odd chain lengths.

4.1.2. Clearing point

The clearing point is determined by the stability of the smectic phase. We have found three factors which affect the smectic phase stability and thus the clearing point.

4.1.2.1. Chainlength

As the alkyl chain length increases from α-C_8Man to α-C_{10}Man and then to α-C_{12}Man, the clearing point rises from 132°C through 149°C to 157°C. Similar increases are seen for other homologous series [7, 32]. Thus a longer chain length leads to a higher clearing point. To understand why this is so, we should remember that it is the rod-like nature of a molecule which gives
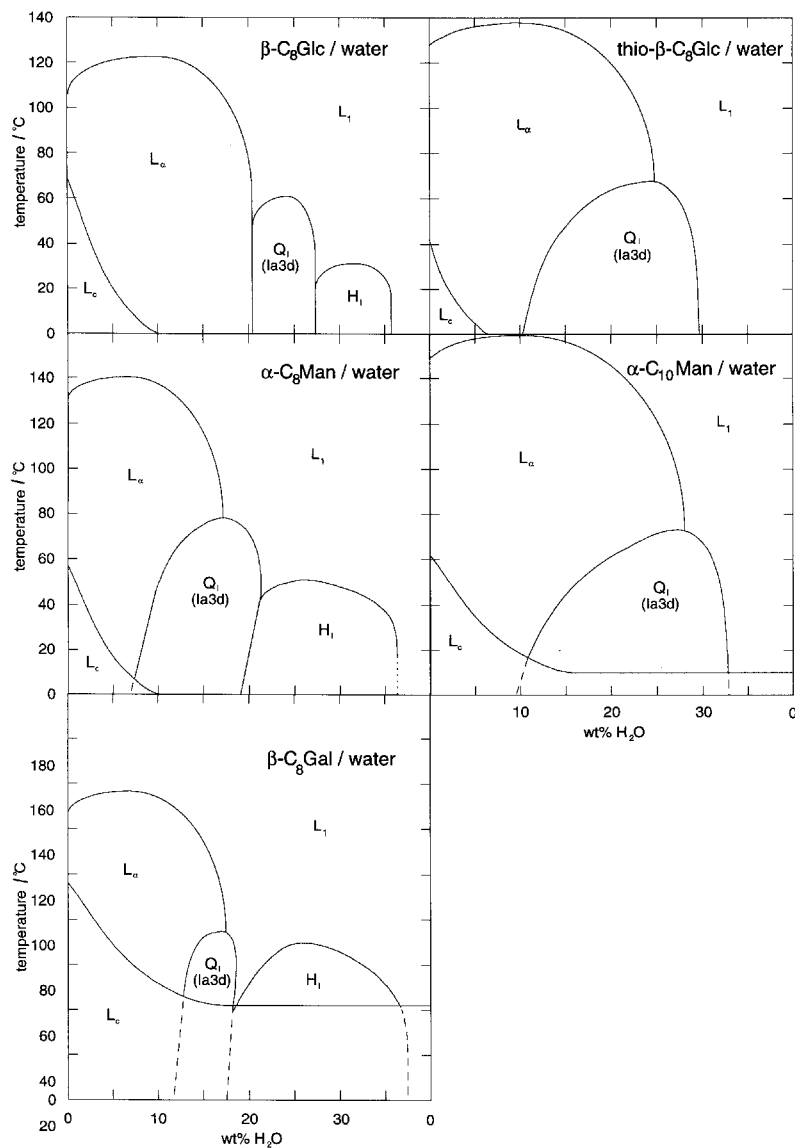
Figure 9. The binary phase diagrams in water of β-C$_8$Glc, thio-β-C$_8$Glc, α-C$_8$Man, α-C$_{10}$Man, and β-C$_8$Gal.

it liquid crystalline properties. As the alkyl chain of a glycoside is lengthened, the molecule becomes longer and more rod-like, and so the smectic phase is stabilized. For chain lengths greater than C$_{12}$, the situation may become more complex, with other factors coming into play [33].

The increase in clearing point with chain length does also suggest that the alkyl chain groups in the smectic phase do still retain *some* degree of interaction with each other. Accordingly, the chain groups should be considered as 'partially melted' rather than completely melted.

4.1.2.2. Intermolecular hydrogen bonding

We can now picture the smectic phase as bilayers of molecules, with dynamically hydrogen bonded head groups on the outside, and partially melted, interdigit-

ated alkyl chains on the inside. As temperature increases, the molecules vibrate more and more vigorously, until a point is reached when the vibrations are strong enough for the molecules to break away from each other, thus destroying the smectic structure. This is the clearing point, when the enthalpic cost of breaking the interactions between the molecules is met by the gain in entropy of going from an ordered to a disordered system.

Hydrogen bonds between the head groups are the main interactions between molecules in the smectic phase. However, although it is commonly accepted that intermolecular hydrogen bonding is crucial in determining thermotropic properties, there has been little progress in relating thermotropic behaviour to molecular structure. Van Doren & Wingert [31] suggest that the hydroxyl groups on the sugar head group serve two
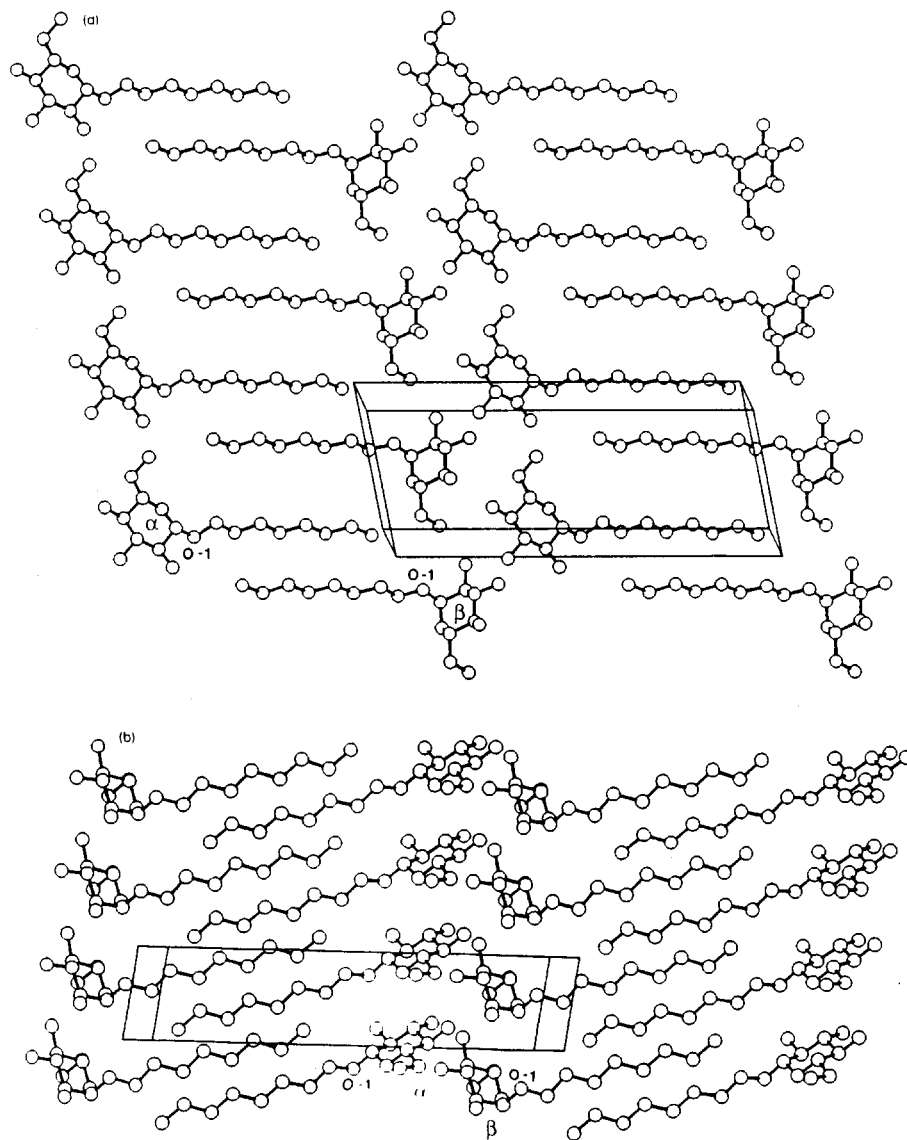
Figure 10. The molecular packing in the crystal structure of a 1:1 binary mixture of α-C$_8$Glc and β-C$_8$Glc; taken from reference [28].

purposes: the hydroxyls near the end of the head group and furthest from the chain group allow the molecule to hydrogen bond to opposing layers, stabilizing the smectic layering, while the hydroxyls on the sides of the head group and nearer to the chain group serve to hold together the molecules within each layer. They also noted that for five acyclic carbohydrates of the same chain length, the clearing point rises as the hydrogen bonding ability of the polar groups increases.

In order to understand precisely the hydrogen bonding that is present in the smectic phase, we need the crystal structures of the compounds under study, and also computer models to help us visualize the complex three-dimensional interactions that take place. Without these, there is only a limited amount we can say about hydrogen bonding interactions.

β-C$_8$Gal has a clearing point of 127°C, whereas β-C$_8$Glc has a clearing point of 107°C. Both molecules possess four hydroxyl groups and two ether-linked oxygen atoms. The only difference between these molecules is that the C4-linked hydroxyl group is axial in β-C$_8$Gal, but equatorial in β-C$_8$Glc. We suggest that this difference affects the ratio of *inter*molecular to *intra*molecular hydrogen bonding which takes place. One possibility is that the axial C4 hydroxyl of β-C$_8$Gal sticks out of the plane of the sugar ring and so is more likely to interact with adjacent molecules, thus increasing the clearing point. However, it should be pointed out that dynamical packing effects [10] could also be invoked to explain this difference.

The clearing point of thio-β-C$_8$Glc (126°C) is also substantially higher than that of β-C$_8$Glc (107°C).

Whereas the bridging oxygen atom in β-C$_8$Glc can participate in hydrogen bonding, the bridging sulphur atom of thio-β-C$_8$Glc cannot. We suggest that this difference again affects the degree of intermolecular hydrogen bonding which takes place, although we cannot pinpoint the specific interactions which are involved.

Let us compare these structures with those of α-C$_8$Fuc and β-C$_8$Fuc (figure 1). Both these molecules have only three hydroxyl groups, rather than four. Carbon 6 acts as a hydrophobic methyl 'spacer' which repels polar groups on adjacent molecules and so reduces the interactions between head groups. The crystal layer spacing of α-C$_8$Fuc suggests that it packs in monolayers rather than bilayers. It appears that, in the crystal phase, the head groups are insufficiently polar and the intermolecular hydrogen bonding interactions are too weak to bring the head groups of opposing monolayers together to form a bilayer structure. Without such a bilayer structure in the crystal phase, the smectic phase cannot be formed. So at the melting point both the chain groups and the head groups melt, and the solid changes directly into an isotropic liquid.

4.1.2.3. *α- and β-anomers*

The α-anomers α-C$_8$Glc and α-C$_8$Man have higher clearing points than the β-anomers β-C$_8$Glc and β-C$_8$Gal. Table 3 shows that the smectic phase layer spacings of the α-anomers are smaller than those of the β-anomers. The decrease in the angle of the sugar ring to the alkyl chain in the α-anomer appears to shorten the molecule (compare α-C$_8$Glc and β-C$_8$Glc in figure 1). We suggest that it also, by introducing a 'kink' in the molecule, increases the lateral spacing between chain groups. Whereas in the comparatively flat β-C$_8$Glc structure there is little room for the chain groups to vibrate, and so they eventually push each other apart and destroy the smectic structure, there is greater space for the chain groups of the α-anomers to vibrate, and so the smectic phase is stable to higher temperatures.

4.2. *Lyotropic properties*

4.2.1. *Solubility in water*

To have any lyotropic properties at all, a surfactant must be sufficiently hydrophilic that the head group interacts with water. The solvation process involves the formation of a complete hydration shell around the polar head group of the molecule. The water is attracted to polar groups on the head group, in particular the hydroxyl groups. Thus there must be enough hydroxyl groups to attract the water to the head group, and these hydroxyl groups must be arranged so that the water can form a complete hydration shell around the head group.

Whereas all the other glycosides studied here possess four hydroxyl groups, α-C$_8$Fuc and β-C$_8$Fuc both contain only three hydroxyl groups. The presence of the hydrophobic methyl group on the sugar ring reduces the hydrophilicity of the head group, and also diminishes the difference in polarity between the head group and chain regions.

It is more difficult to explain why α-C$_8$Man is soluble in water whereas α-C$_8$Glc is not. Both molecules possess four hydroxyl groups, and the only difference in their structures is that the C2-linked OH is axial in α-C$_8$Man and equatorial in α-C$_8$Glc.

The crystal structure of α-C$_8$Glc has been solved [26, 27]. There is a strong hydrogen bonding network between opposing bilayers. Water molecules are attracted into voids between the bilayers and become part of this hydrogen bonding network. However, there appears to be insufficient hydrophilicity closer to the chain group to allow a complete hydration shell to form around the head group. Instead, the water molecules remain trapped in the voids between the bilayers, forming a stable crystalline hemihydrate and monohydrate. In contrast, the axial C2-linked OH in α-C$_8$Man appears to modify the crystal structure, allowing a hydration shell to form around the head group, and thus making the molecule soluble.
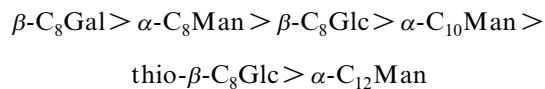
4.2.2. *Extent of the lamellar and curved phases*

In all the lyotropic systems studied, the thermal stability of the fluid lamellar L$_\alpha$ phase rises when water is added, up to a maximum at approximately 8–10 wt % water. This is because, at low hydrations, water molecules which are added participate in the hydrogen bonding network between the head groups, strengthening the interactions between them and thus increasing the rigidity of the lamellar phase.

From table 2 one can see that the stability of the lamellar phase is closely related to the stability of the smectic A phase. This probably reflects the fact that the two phases have a similar bilayer structure, with partially melted chain groups. Comparison of the smectic and lamellar layer spacings (tables 3 and 4) shows that the lamellar spacings are similar to, but slightly larger than, the smectic spacings, owing to the presence of hydrogen bonded water molecules around the head groups.

The extent of curved phases in the phase diagram depends on the ratio of head group volume to chain group volume. The larger the volume of the head group relative to the chain group, the greater the desire for positive interfacial curvature, and the greater the extent of curved phases.

If we look at the trend in curvature over the five phase diagrams (figure 9), we find the following series (note that α-C$_{12}$Man forms only the lamellar phase, table 4, and thus has the least interfacial curvature of all of

these compounds), with curvature decreasing from left to right:

$$\beta\text{-}C_8\text{Gal} > \alpha\text{-}C_8\text{Man} > \beta\text{-}C_8\text{Glc} > \alpha\text{-}C_{10}\text{Man} >$$

$$\text{thio-}\beta\text{-}C_8\text{Glc} > \alpha\text{-}C_{12}\text{Man}$$

This *curvature series*, with the $\beta\text{-}C_8\text{Gal}$/water and $\alpha\text{-}C_8\text{Man}$/water systems exhibiting the most curvature and the $\alpha\text{-}C_{12}\text{Man}$/water system the least, closely matches the trend in the molecular breadth/length ratio. The larger the breadth of the molecule relative to its length, the greater the desire for curvature.

Three compounds exhibited lamellar, cubic and hexagonal phases in the same phase diagram. $\beta\text{-}C_8\text{Gal}$ has the largest area of hexagonal phase, stable between 18% and 37% water (25°C) and up to 70°C, but a smaller area of cubic phase, while $\alpha\text{-}C_8\text{Man}$ has a larger area of cubic phase and a smaller region of hexagonal phase. In comparison, $\beta\text{-}C_8\text{Glc}$ also exhibits both cubic and hexagonal phases, but the area covered by these phases in the phase diagram is less.

All three molecules have small, *n*-octyl chains and large pyranoside head groups. However, in $\beta\text{-}C_8\text{Glc}$ the head group, though large, is fairly flat. In contrast, the axial, C4-linked hydroxyl group of $\beta\text{-}C_8\text{Gal}$ both shortens the molecule and also points outwards from the structure, increasing the head group width relative to $\beta\text{-}C_8\text{Glc}$. Likewise, the α-linkage makes the $\alpha\text{-}C_8\text{Man}$ head group shorter and wider than the $\beta\text{-}C_8\text{Glc}$ head group, thus raising the molecular breadth/length ratio, and increasing the desire for curvature.

The predictable decrease in curvature from $\alpha\text{-}C_8\text{Man}$ to $\alpha\text{-}C_{10}\text{Man}$ and then to $\alpha\text{-}C_{12}\text{Man}$ is clearly due to the increase in alkyl chain length, which makes the molecule more rod-like and so less likely to form curved phases.

More surprising is the observation that the lyotropic phase behaviour of $\alpha\text{-}C_{10}\text{Man}$ and thio-$\beta\text{-}C_8\text{Glc}$ is very similar. The phase diagrams of both molecules exhibit large areas of lamellar and cubic phase, but no hexagonal phase. Interestingly, the change in phase behaviour on going from $\beta\text{-}C_8\text{Glc}$ to thio-$\beta\text{-}C_8\text{Glc}$ is similar to the change from $\alpha\text{-}C_8\text{Man}$ to $\alpha\text{-}C_{10}\text{Man}$. Thus the substitution of a bridging sulphur (thio-$\beta\text{-}C_8\text{Glc}$) for a bridging oxygen ($\beta\text{-}C_8\text{Glc}$) has nearly the same effect on lyotropic properties as increasing alkyl chain length by two carbon atoms. This is probably because the bridging oxygen in $\beta\text{-}C_8\text{Glc}$ takes part in the intermolecular hydrogen bonding network, is included in the hydration sphere, and is thus effectively part of the head group, whereas the bridging sulphur in thio-$\beta\text{-}C_8\text{Glc}$ does not hydrogen bond, and so acts as part of the chain group. So, relative to $\beta\text{-}C_8\text{Glc}$, thio-$\beta\text{-}C_8\text{Glc}$ has both a smaller head group and a longer chain group.

4.3. *Summary*

Having analysed qualitatively the factors which determine the thermotropic and lyotropic phase behaviour of alkyl glycosides, we now briefly summarize the effects of the various structural modifications.

4.3.1. *α- and β-anomers*

The smectic and lyotropic phases of the α-anomers are more thermally stable than those of the β-anomers, presumably because the α-anomers have stronger lateral bonding between the head groups. The α-anomer also has a larger breadth/length ratio than the β-anomer, and so the desire for positive interfacial curvature is greater.

4.3.2. *Chain length*

Increasing chain length leads to a gradually increasing melting point and a more rapidly increasing clearing point, as the molecule becomes more rod-like, stabilizing the smectic A phase. Increasing the chain length also reduces the breadth of the molecule relative to its length, reducing the desire for curvature and the extent of curved lyotropic phases.

4.3.3. *Bridging atom*

If the oxygen which links the sugar ring to the alkyl chain is replaced by a sulphur, the melting point is lowered and the clearing point is raised. Because the bridging oxygen in $\beta\text{-}C_8\text{Glc}$ participates in the hydrogen bonding network, it is effectively part of the polar head group. In contrast, the bridging sulphur in thio-$\beta\text{-}C_8\text{Glc}$ does not participate in hydrogen bonding and so is part of the non-polar chain group. Thus the thio substitution reduces the effective size of the head group, and has the same effect on lyotropic properties as increasing the chain length by two carbons. The thio derivative has, consequently, a lesser desire for interfacial curvature.

4.3.4. *Number and arrangement of hydroxyl groups in the sugar ring*

If there are too few OH groups on the sugar ring (e.g. $\alpha\text{-}C_8\text{Fuc}$ and $\beta\text{-}C_8\text{Fuc}$) there will be insufficient intermolecular hydrogen bonding to form a smectic phase, and the solubility in water will be low. For the molecule to be soluble in water, the arrangement of hydroxyl groups must allow a hydration shell to form around the head group.

The configuration of the hydroxyl groups in the ring can also affect the ratio of inter- and intramolecular hydrogen bonding. The greater the extent of intermolecular hydrogen bonding, the greater is the stability of the smectic and lamellar phases.

5. Conclusions

We have examined the thermotropic and lyotropic phase behaviour of a series of seven monoalkyl glycosides, and compared them with two previously studied [1] glycoside surfactants. β-C$_8$Glc, β-C$_8$Gal and α-C$_8$Man exhibit smectic A phases when dry and type I lamellar, cubic and hexagonal phases on the addition of water. α-C$_{10}$Man and thio-β-C$_8$Glc exhibit smectic, lamellar and cubic phases, but no hexagonal phase. Although α-C$_8$Glc and α-C$_{12}$Man both form smectic phases when dry, the crystalline forms of these compounds are insoluble in water. However, when water is added to the smectic phase of either of these glycosides, the lamellar phase is formed. α-C$_8$Fuc and β-C$_8$Fuc showed no thermotropic or lyotropic properties at all.

The important effect of intermolecular hydrogen bonding on the phase behaviour of alkyl glycosides has been a central theme of this study. Our knowledge of the hydrogen bonding which takes place between glycoside molecules is still incomplete. Without an intimate understanding of these interactions we cannot explain how structural modifications such as changes in the arrangement of OH groups on the sugar ring affect phase behaviour. To gain such an understanding we would need the crystal structures of these molecules, as well as computer modelling of their intermolecular interactions. Nonetheless, this comparative study has provided a large amount of useful new information. The effect of substituting a sulphur atom for the bridging oxygen atom is particularly interesting, and this aspect of the study could usefully be extended to see whether the thio derivative of α-C$_8$Man would produce the same phase behaviour as α-C$_{10}$Man, as one might expect. The thio derivatives of β-C$_8$Gal and α-C$_8$Man could be synthesized, as could many other related compounds, such as α-C$_8$Gal, and β-C$_8$Man. Indeed, there are many related glycoside compounds which have already been synthesized, and whose thermotropic properties have been reported, but whose lyotropic properties remain to be characterized.

References

[1] SAKYA, P., SEDDON, J. M., and TEMPLER, R. H., 1994, *J. Phys. II France*, **4**, 1311.

[2] CHUNG, Y. J., and JEFFREY, G. A., 1989, *Biochim. Biophys. Acta*, **985**, 300.

[3] LUZZATI, V., 1995, *J. Phys. II France*, **5**, 1649.

[4] NILSSON, F., SÖDERMAN, O., and JOHANSSON, I., 1996, *Langmuir*, **12**, 902.

[5] JEFFREY, G. A., 1984, *Mol. Cryst. Liq. Cryst.*, **110**, 221.

[6] JEFFREY, G. A., and WINGERT, L. M., 1992, *Liq. Cryst.*, **12**, 179.

[7] PRADE, H., MIETCHEN, R., and VILL, V., 1995, *J. Prakt. Chem.*, **337**, 427.

[8] GOODBY, J. W., 1984, *Mol. Cryst. Liq. Cryst.*, **110**, 205.

[9] DORSET, D. L., 1990, *Carbohydr. Res.*, **206**, 193.

[10] VILL, V., BÖCKER, T., THIEM, J., and FISCHER, F., 1989, *Liq. Cryst.*, **6**, 349.

[11] VAN DOREN, H. A., VAN DER GEEST, R., and RUIJTER, C. F., 1990, *Liq. Cryst.*, **8**, 109.

[12] KOYNOVA, R., and CAFFREY, M., 1994, *Chem. Phys. Lipids*, **69**, 181.

[13] MICHEL, H., and OESTERHELT, D., 1980, *Proc. Natl. Acad. Sci. USA*, **77**, 1283.

[14] GARAVITO, R. M., and ROSENBUSCH, J. P., 1980, *J. Cell Biol.*, **86**, 327.

[15] SHINODA, K., CARLSSON, A., and LINDMAN, B., 1996, *Adv. Coll. Interface Sci.*, **64**, 253.

[16] MATSUMURA, S., IMAI, K., YOSHIKAWA, S., KAWADA, K., and UCHIBORI, T., 1990, *J. Am. Oil Chem. Soc.*, **67**, 996.

[17] LOEWENSTEIN, A., IGNER, D., ZEHAVI, U., ZIMMERMANN, H., EMERSON, A., and LUCKHURST, G. R., 1990, *Liq. Cryst.*, **7**, 457.

[18] LOEWENSTEIN, A., and IGNER, D., 1991, *Liq. Cryst.*, **10**, 457.

[19] LOEWENSTEIN, A., and IGNER, D., 1993, *Liq. Cryst.*, **13**, 531.

[20] MITCHELL, D. J., TIDDY, G., WARING, L., BOSTOCK, T., and McDONALD, M. P., 1969, *J. Chem. Soc. Faraday Trans., I*, **79**, 975.

[21] RANÇON, Y., and CHARVOLIN, J., 1988, *J. Phys. Chem.*, **92**, 2646.

[22] RANÇON, Y., and CHARVOLIN, J., 1988, *J. Phys. Chem.*, **92**, 6339.

[23] CLERC, M., LEVELUT, A. M., and SADOC, J. F., 1990, *Colloque de Phys.*, **51**, 97.

[24] CLERC, M., LEVELUT, A. M., and SADOC, J. F., 1991, *J. Phys. II France*, **1**, 1263.

[25] VILL, V., LINDHORST, T., and THIEM, J., 1991, *J. Carbohydr. Chem.*, **10**, 771.

[26] JEFFREY, G. A., and YEON, Y., 1987, *Carbohydr. Res.*, **169**, 1.

[27] VAN KONINGSVELD, H., JANSEN, J. C., and STRAATHOF, A. J. J., 1988, *Acta Cryst.*, **C44**, 1054.

[28] JEFFREY, G. A., and YEON, Y., 1992, *Carbohydr. Res.*, **237**, 45.

[29] CARTER, D. C., RUBLE, J. R., and JEFFREY, G. A., 1982, *Carbohydr. Res.*, **102**, 59.

[30] JEFFREY, G. A., and MALUSZYNSKA, H., 1990, *Carbohydr. Res.*, **207**, 211.

[31] VAN DOREN, H. A., and WINGERT, L. M., 1991, *Mol. Cryst. Liq. Cryst.*, **198**, 381.

[32] JEFFREY, G. A., 1986, *Acc. Chem. Res.*, **19**, 168.

[33] VILL, V., KELKENBERG, H., and THIEM, J., 1992, *Liq. Cryst.*, **11**, 459.